Electrochimica Acta 403 (2022) 139609

Contents lists available at ScienceDirect

Electrochimica Acta

journal homepage: www.elsevier.com/locate/electacta

An electrochemically switched ion exchange α-ZrP/PPy film as a synergistically catalytic and anchoring material towards lithium-sulfur battery design

Wei Zhang[a], Ye Liu[a], Ailian Wu[a,**], Lixia Ling[a,**], Zhongde Wang[a,*], Xiaogang Hao[a], Guoqing Guan[b]

[a] Department of Chemical Engineering, Taiyuan University of Technology, Taiyuan, 030024, China
[b] Department of Renewable Energy Institute of Regional Innovation, Hirosaki University, 2-1-3, Matsubara, Aomori 030-0813, Japan

ARTICLE INFO

Article history:
Received 23 May 2021
Revised 8 November 2021
Accepted 15 November 2021
Available online 18 November 2021

Keywords:
Li-S batteries
α-zirconium phosphate/polypyrrole
Density functional theory calculation
Electrocatalysis
Polysulfide

ABSTRACT

The commercial application of lithium-sulfur (Li-S) batteries is largely hindered by their insufficient rate performance and cycle stability because of the shuttle effect and sluggish kinetic conversion of lithium polysulfides (LiPSs). Herein, an electrochemically switched ion exchange film of heterostructured α-zirconium phosphate/polypyrrole (α-ZrP/PPy), which combined the virtues of conductive PPy with highly adsorptive α-ZrP was investigated to be able to synergistically restrain the shuttle effect and facilitate the redox reaction kinetics of LiPSs by employing the density functional theory (DFT) calculation. The mechanism of redox reaction and the microcosmic-properties of electron were explored in detail. Adsorption calculations revealed that the captured LiPSs by α-ZrP/PPy with a moderate adsorption ability and the electrocatalytic activity of the anchoring material would effectively restrain the shuttle effect and accelerate the decomposition of LiPSs back to sulfur during charging process. Furthermore, α-ZrP and PPy provided unique ion migration channel and electronic transfer channel, respectively, and the rapid redox reactions were induced by excellent surface diffusion of lithium ion in the interface of α-ZrP/PPy. Particularly, the charge differential density uncovered that LiPSs served as an accurate regulable-switch tune the electronic transfer in the redox reactions relating to α-ZrP and PPy. Thus, the α-ZrP/PPy based cathode owned outstanding adsorption capacity as well as electric catalytic properties in the Li-S batteries.

1. Introduction

Lithium ion batteries have been deemed as an efficient energy storage system in various power grids in recent years [1,2]. However, there are significant issues raised by high cost and the limited theoretical specific capacity of ~300 mA h g^{-1}, which cannot fulfill some urgent needs of energy storage [3,4]. Fortunately, lithium-sulfur (Li-S) batteries with the sulfur cathode have an energy density of up to 2600 mA h g^{-1}, which is 3 to 5 times higher than that of traditional lithium batteries and is expected to be the next-generation batteries [5–7]. Nevertheless, their practical application is still hindered by the volume expansion, the kinetic delay, the insulating sulfur and Li_2S (Li_2S_2) and the shuttling of intermediates in electrolytes [8,9].

To ameliorate the issues of volume expansion and low electrical conductivity insulating sulfur and Li_2S (Li_2S_2), extensive researches have demonstrated that the incorporation of sulfur into carbon materials (e.g., carbon nanotubes [10,11], carbon fibers [12], and graphene [13]) and conductive polymers [14] and their hybrids [15] as anode protectors and conductive additives. In addition to the experimental characterization, density functional theory (DFT) calculation also plays an indispensable role for exploring appropriate anchoring materials. The calculated results showed that the weak physical interaction between the carbon material and LiPSs caused shuttle effect, which limits the improvement in the cycling performance of Li-S batteries [16,17]. To avoid the shuttling effect, recently, it is found that polar materials with abundant polar surfaces such as metal-based composites (e.g., metal sulfides, metal oxides, metal carbides and metal nitrides) can anchor LiPSs more strongly with larger chemical adsorption energies, which could render Li-S batteries with admirable cycle immobility and reversibility [18–20]. Although the incorporation of sulfur into polar materials could achieve excellent cycle stability, the converting of Li_2S into insoluble S_8 is still kinetically sluggish. The

* Corresponding author.
** Corresponding authors.
E-mail addresses: wuailian@tyut.edu.cn (A. Wu), linglixia@tyut.edu.cn (L. Ling), wangzhongde@tyut.edu.cn, zdwangtyut@hotmail.com (Z. Wang).

https://doi.org/10.1016/j.electacta.2021.139609
0013-4686/

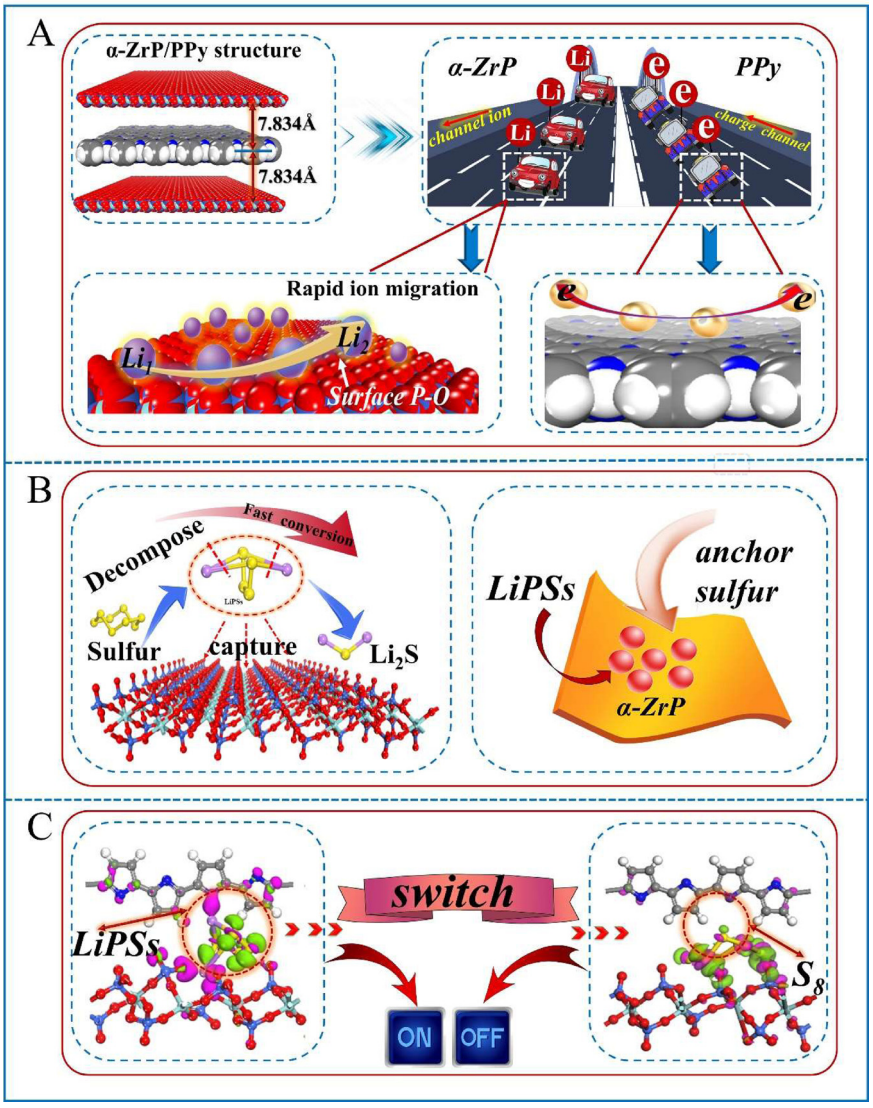

Fig. 1. Schematic illustration of the capture of sulfur species and the catalysis of LiPSs conversion based on α-ZrP/PPy host.

calculated results manifested that the lower Li_2S decomposition energy barrier of those activation materials could facilitate Li_2S back to sulfur, which would hinder the charging/discharging process once Li_2S is deposited on the electrode surface [21,22]. The intermediates reduction process contains two steps: immobilization and electrochemical conversion of LiPSs involving a complex multi-electron reactions and phase transitions [9,20,23,24]. Consequently, the accelerating of redox reaction by the catalysis of anchoring materials would improve the reversibility of Li-S batteries. Such a strategy has a great inspiration in the material design.

As a high-efficient electrochemically switched ion exchange material with a two-dimensional layered structure, α-ZrP has large specific surface area and unique surface charge and has been attracted comprehensive exploration [25], which could be a promising candidate cathode material for Li-S batteries. Meanwhile, for an ideal anchoring material, it should possess excellent conductivity [9,26]. For example, PPy has high ion and electron transportation ability. In addition, to adjust the electronic properties, preparation of cathode material with heterostructure is also important. For example, such a material was successfully prepared by compositing of layered α-ZrP nanosheets with conductive polyaniline (PANI) chains, which exhibited fast uptake/release ability with high capacity [27,28]. Moreover, this material exhibited not only high electrical activity [27] but also a long-term cycle stability [25,28]. Based on these results, the α-ZrP/PPy composite with a sandwiched structure was innovatively designed as a new battery cathode material, which effectively improved the electrical conductivity of the overall material [29]. However, there is little reported information about the path of the electron or ion transfer and decomposition barrier of polysulfides, which is difficult to validate experimentally. The redox reaction mechanism of α-ZrP/PPy needs to be further investigated. Density functional theory has been identified as a better systematic analysis tool to offer accuracy evidence to reveal the microcosmic-properties of electron variation and ion migrate process at the molecular level [16,17,20,21].

In this contribution, the density functional theory was employed to dissect the internal feasibility factor of α-ZrP/PPy as the cathode material of Li-S battery. Herein, the adsorption energy, electronic property, diffusion barrier of lithium ions and decomposition barrier of LiPSs in α-ZrP/PPy interface were obtained as the basis for analysis. Schematic illustration on the capture of sulfur species and the catalysis of LiPSs conversion based on the theoretical simulation is shown in Fig. 1, in which PPy acts as an electron transfer channel to effectively reduce the impedance of charge transport within the cathode whereas α-ZrP employs as an ion transfer channel to promote the redox reaction. As such, PPy

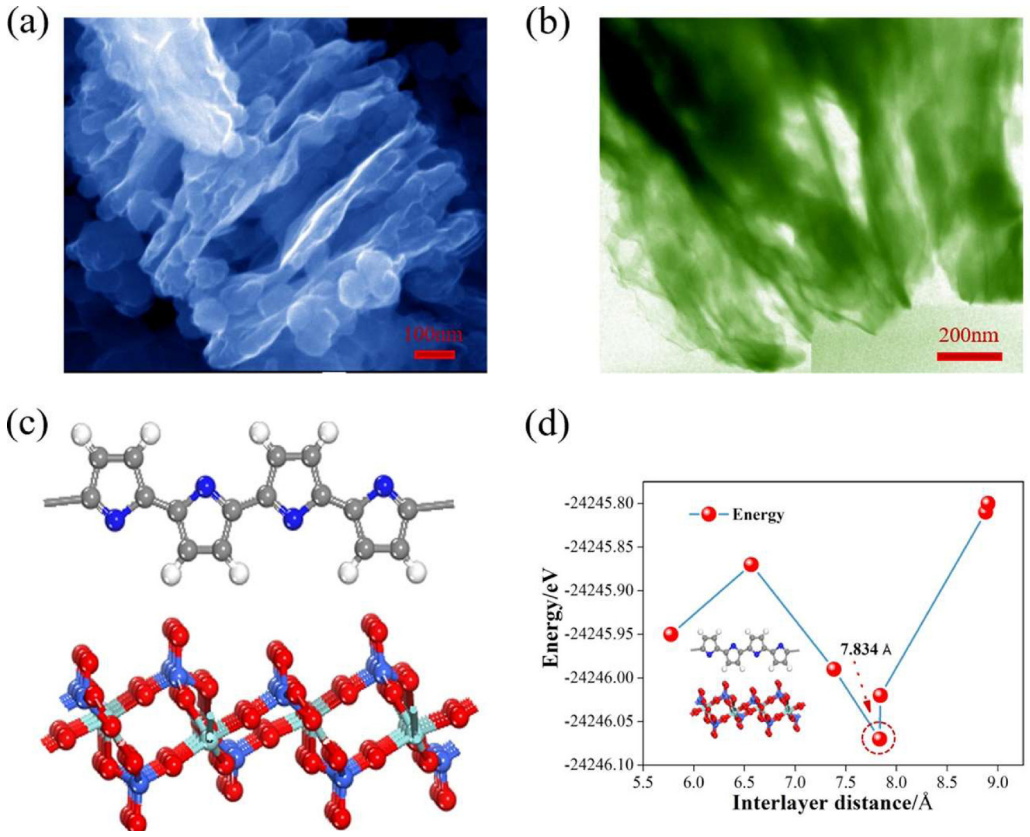

Fig. 2. (a) SEM and (b) TEM images of the as-prepared α-ZrP/PPy. (c) Optimized structure of α-ZrP/PPy. (d) The energy evolution as a function of interlayer distance d between α-ZrP and PPy.

and α-ZrP could synergistically cause a highest chemical adsorption energy for LiPSs on α-ZrP/PPy, which can tackle the shuttle effect and thereby generating a stable cycle performance (Fig. 1A). Interestingly, LiPSs can serve as an electronic switch for tuning the electronic transfer between α-ZrP and PPy, accelerating the redox reaction (Fig. 1C), which helps to realize the fast capture, conversion and decompose of LiPSs in the α-ZrP/PPy interface (Fig. 1B). As expected, a small decomposition barrier of 0.54 eV for Li_2S was achieved for the α-ZrP/PPy, which could accelerate the redox kinetics. This work deepens the understanding of the unique electrochemically switched ion exchange material as the polar sulfur hosts, and could stimulate more experimental and theoretical explorations to develop Li-S batteries with superb performance.

2. Theoretical approach

The DFT calculations were performed by using the CASTEP (Cambridge Serial Total Package) code included in Materials Studio 8.0 software package of Accelrys (Inc., San Diego. CA) [30]. The geometric and electronic structures of the α-ZrP/PPy model were calculated using the plane wave pseudopotential method. The electron exchange function was employed by Perdew-Burke-Ernzerhof (PBE) [31] described by the generalized gradient approximation (GGA) [32]. The α-ZrP/PPy heterostructure was modeled by a supercell, which contains $p(2 \times 1)$ [33] α-ZrP units of (0 0 1) surface and $p(4 \times 1)$ polymer units of PPy [25]. To avoid the interaction between adjacent layers, the vacuum layer distance was built to 25 Å [9]. Also, van der Waals interaction between different LiPSs species and the anchoring materials were treated by DFT-D2 correction [33]. Moreover, the ultrasoft pseudopotential of each atom and energy cutoff of 340 eV for plane-wave expansion were used during the self-consistent field (SCF) calculation [34]. We ensure that all geometric configurations were under full relaxation. The convergence criteria acting on each ion in the maximum force, maximum pressure and maximum displacement were employed at 10^{-5} eV, 0.03 eV $Å^{-1}$, 0.05 GPa, 10^{-3} Å, respectively. The electronic self-consistent field (SCF) tolerance was set at 10^{-6} eV $atom^{-1}$ and the *k*-point in Brillouin region selected by Monkhorts-Pack method was adopted at $2 \times 2 \times 1$ [35]. In the calculation of lithium ions diffusion barrier and LiPSs decomposition, the methods of complete linear synchronous transit (LST) and quadratic synchronous transit (QST) were implemented to calculate the minimum energy path (MEP) of the diffusion and decomposition process to locate the transition state [36]. Firstly, a series of image structures were inserted between the initial and final states of the reaction, and then artificial spring force was introduced between all the nearest neighbor image structures to obtain MEP [37]. The RMS convergence rate was 0.05 eV $Å^{-1}$. The energy difference between the initial state and the saddle point was defined as the diffusion barrier.

3. Results and discussion

3.1. Structures and stabilities of anchoring materials, S_8 cluster and LiPSs

2D layered α-ZrP/PPy material was prepared with a simple facile exfoliated-stacked strategy, the detailed method is consistent with previous research [29]. From the scanning electron microscope (SEM) image (Fig. 2a), one can see that the α-ZrP/PPy composite had a stacked 2D layered structure. From the high resolution transmission electron microscopy (HRTEM) image, PPy was found to be uniformly distributed on the 2D α-ZrP nanosheets, forming a layered sandwich structure (Fig. 2b).

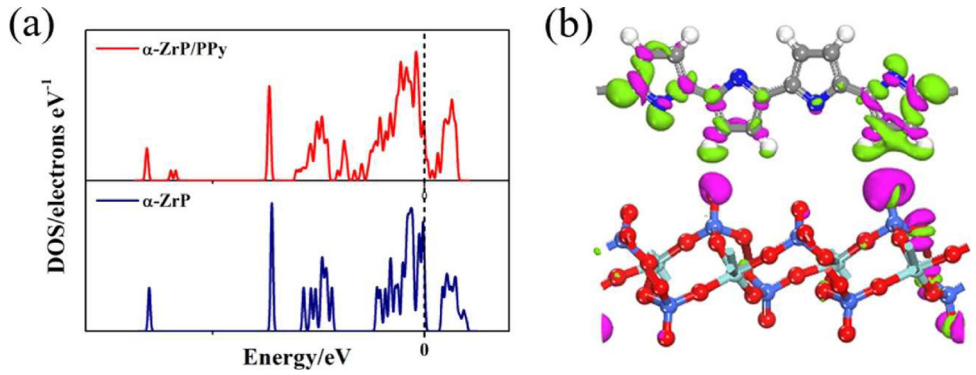

Fig. 3. (a) DOS of α-ZrP/PPy and α-ZrP. The dashed line refers to the Fermi level. (b) Charge transfer between α-ZrP and PPy. The charge transfer can be defined as $\Delta\rho=\rho(AM+Li_2S_n)-\rho(AM)-\rho(Li_2S_n)$, where $\rho(AM+Li_2S_n)$, $\rho(AM)$, and $\rho(Li_2S_n)$ are the charge densities for anchoring system, α-ZrP/PPy (AM) system, and LiPSs system, respectively. Here, pink (green) is the spatial regions gain (loss) in charge. (For interpretation of the references to color in this figure legend, the reader is referred to the web version of this article.)

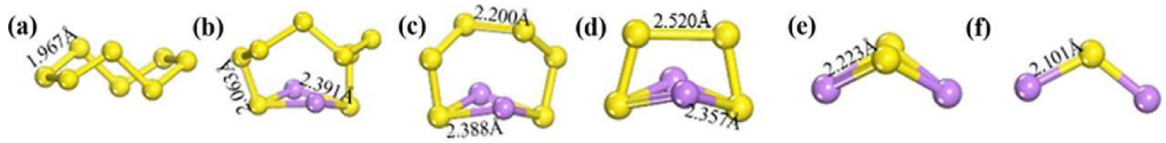

Fig. 4. (a-f) Molecule configurations for Li-S composites at various lithiation stages, from unlithiated S_8 to Li_2S. Here, yellow and purple balls symbolize sulfur and lithium atoms, respectively. (For interpretation of the references to color in this figure legend, the reader is referred to the web version of this article.)

In this work, α-ZrP/PPy composite structure was constructed, where a 2 × 1 × 1 α-ZrP supercell and a PPy layer of four pyrrole units were applied to avoid the mutual repulsion of polysulfides between adjacent unit cells. The lattice mismatch between the α-ZrP layer and PPy layer in the x-y direction was all less than 5%, which was acceptable [9] We considered coating the PPy layer on the surface of the outer layer of α-ZrP in parallel or vertical, respectively. The results reveal that the PPy prefers to be arranged on the α-ZrP parallelly (Fig. 2c). Generally, the interlayer spacing (d) should be the shortest distance between α-ZrP and PPy [9]. As illustrated in Fig. 2d, the value of d is approximately 7.834 Å, implying an exceptional tolerance in diverse LiPSs for the redox reaction of the electrode material even though the S-S bond length is 5.700 Å in the longest chain Li_2S_8 in LiPSs. The density of states of α-ZrP and α-ZrP/PPy is presented in Fig. 3a. The total DOS of the structure demonstrated that the orbit of α-ZrP should not cross the fermi level, resulting in a 3.18 eV value of bandgap whereas the orbital of the α-ZrP/PPy crosses the fermi level with the narrow bandgap of 0.08 eV. According to the Eq. (1):

$$\sigma \sim \exp\left(-E_g {k_B}^{-1} T^{-1}\right) \quad (1)$$

[**37,**38] where E_g, k_B and T are the bandgap and Boltzmann's constant, and room temperature respectively [38],the overall conductivity of the system could be greatly enhanced by the order of 10^{52}, which verifies that the addition of PPy increases the conductivity of the cathode material, thereby increasing the utilization of the cathode active material and improving the rate performance of the battery. It can be deemed to that the combination of α-ZrP and PPy should be an effective way to improve the electrical performance of Li-S battery electrodes. The charge differential density further reveals that there is a significant charge transfer between α-ZrP and PPy (Fig. 3b). It is observed that the charge can be shifted from PPy to the α-ZrP surface, resulting in the deposition of abundant electrons to enhance the activity of α-ZrP and form a built-in electric field [39], which is the reason why the overall material became more conductive.

In the Li-S battery, α-S_8 serves as the most stable allotrope with a crown shape among all the sulfur atoms in the electrode at room temperature. Experiments have confirmed that Li_2S_8, Li_2S_6, Li_2S_4, Li_2S_2, Li_2S would be formed during the discharge process in the presence of extra Li ions. Fig. 4 illustrates molecule configurations for Li-S composites at various lithiation stages from Li_2S_n species (n = 8, 6, 4, 2) to Li_2S, which are in accordance with previous references [17]. All LiPSs own a three-dimensional cluster shape rather than a chain with Li atom on the terminal [9]. Intuitively, the S-S bond lengths of the long-chain Li_2S_n (n = 4, 6, 8) are markedly shorter than those of the short-chain Li_2S_n (n = 1, 2) cluster. Meanwhile, the length of the Li-S bond enlarges with the increase of the number of S atoms. Consequently, in the electrolyte, short-chain Li_2S_2 or Li_2S is more arduous to ionize into lithium ions and sulfur anions than those long-chain Li_2S_n.

3.2. Adsorption of LiPSs in the α-ZrP/PPy interface

The ideal anchoring material in the Li-S battery should possess chemical interaction with those intermediates produced in the battery to inhibit the decomposition of the related substances and shuttle effect during cycling [38]. Thus, the adsorption strength of S_8 cluster or LiPSs in the α-ZrP/PPy heterostructure was first investigated. Herein, the adsorption energy (E_{ads}) was calculated using Eq. (2):

$$E_{ads}=E_{Li_2S_n@AM}-E_{AM}-E_{Li_2S_n} \quad (2)$$

where $E_{Li_2S_n@AM}$, E_{AM}, $E_{Li_2S_n}$ denote the total energies of Li_2S_n+AM, isolated AM, and the summation of pure Li_2S_n, respectively [33]. As such, a negative adsorption energy indicates that the interaction between them is favored. In this work, different configurations of adsorption with respect to S_8 and Li_2S_n in α-ZrP/PPy were considered. We scrutinized the obtained adsorption model structure with the lowest adsorption energy as presented in Fig. 5. The relevant structural parameters and the charge transfer numbers are summarized in Table 1. Taking the adsorption geometry of unlithiated S_8 as an example, the S_8 plane is parallel to the α-ZrP/PPy interface with the shortest S-O distance of 2.929 Å, and the configuration is almost intact. As the lithiation proceeds, it is found that the LiPSs experience stronger structural distortion during the whole reaction process, in which the length of Li-S

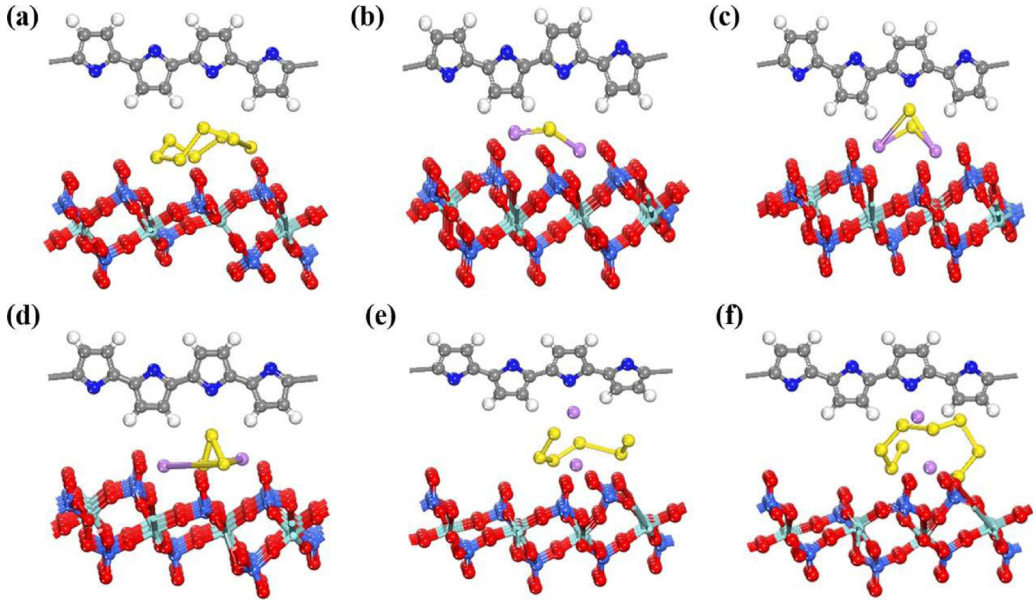

Fig. 5. (a-f) Optimized structures for Li-S composites at six different lithiation stages (S_8, Li_2S, Li_2S_2, Li_2S_4, Li_2S_6, Li_2S_8) in α-ZrP/PPy interface.

Table 1
Computed parameters in the cases of Li_2S and Li_2S_4 cluster adsorbed at the α-ZrP/PPy interface (Li_1, Li_2 and S represent the atoms at the closest interaction positions with O_1, O_2, O_3 of α-ZrP, respectively.).

	d_{Li-S}/Å	$d_{Li_1-O_1(N)}$ /Å	$d_{Li_2-O_2}$/Å	d_{S-O_3}/Å	Δe_{Li_1}	Δe_{Li_2}	Δe_s
Li_2S@α-ZrP/PPy	2.407	1.796	1.914	1.723	0.15	0.09	1.52
Li_2S_4@α-ZrP/PPy	5.397	1.992	1.812	1.699	0.03	0.04	1.04

bond would be enhanced to different extents, intuitively the Li-S bond of long-chain Li_2S_6 is directly elongated by 0.153 Å, indicating the tendency of lithium-sulfur bonds to break. One of the lithium atoms in the long-chain LiPSs prefers to be adsorbed around the N atom of the PPy whereas the other lithium atom with a sulfur atom prefers to attract with the O on the P-O outer layer due to the higher electronegativity of N atom and the chemical activity of the P-O outer layer when compared with those of other atoms. Meanwhile, it is observed that all atoms participate in the electrochemical reaction in the short-chain Li_2S-Li_2S system, in which they are basically unchanged during the reaction highly correlated to the lithium-sulfur bonds shorter than those of other long-chain compounds (2.223 Å and 2.101 Å, respectively). It should be noted that the adsorption strengths are different between high-order LiPSs and low-order LiPSs owing to the different adsorption configurations. From the Fig. 6a, it can be seen that the induced binding energies of S_8, Li_2S_n in α-ZrP/PPy are in the range from −0.69 to −6.24 eV, indicating an excellent adsorption capacity for LiPSs. The magnitude of adsorption energy gradually increases as the number of S atoms decreases. Surprisingly, it is found that the adsorption energy value of Li_2S_n is suddenly increased by more than 1.50 eV when n is changed from 4 to 2 and 1 during the liquid-solid phase transition. This extraordinary increase in the magnitude of change should be caused by the special adsorption characteristics of Li_2S and Li_2S_2, where all lithium and sulfur atoms contribute to the bond-forming in a limited space. Taking Li_2S and Li_2S_4 as the representatives of short-chain LiPSs and long-chain LiPSs, it can be seen from Table 1 that the charge changes of sulfur atoms are larger than those of lithium atoms, resulting in a chemical S-bond and rather weaker Li-bond are formed [17]. At the same time, it is exhibited that the change of sulfur atoms participating in the bond formation increases with the progress of lithiation, which is consistent with the adsorption trend. The additional results are shown in Table S1 of Supporting Information, which can also be understood by the adsorption configuration mentioned above. It is also illustrated that the shortest S-O bond is stretched to 1.699 Å and 1.723 Å after the adsorption of Li_2S and Li_2S_4, respectively, which are as strong as the corresponding bond length in crystal [37], solidifying the so-called chemical bonds. Consequently, the origin of anchoring effect might be mainly dominated by the formation of chemical S-O bonds as well as the relatively weaker interactions afforded by dipole-dipole electrostatic interactions of the so-called “Li bond” in the electrode redox process, which can synergistically catalyze redox reaction [38].

In order to further ascertain the interaction quantitatively, the charge density difference diagram and the changes of Mulliken charge distribution were employed to achieve the quantity of electrons between these intermediates and substrates [40]. Taking adsorption systems of Li_2S_4 and S_8 as examples, which are displayed in Fig. 6c and d. Besides, others are demonstrated in Fig. S1 of the Supporting Information. In the particular case of Li_2S_4, the electron density variations around S and O are relatively insignificant, manifesting a large electronic depletion on the S atom (green part), while the charge accumulates on the adjacent O atom, which induces a chemical S-O bond. The existence of S-O bond could avoid the excessive oxidation of polysulfide. The inhomogeneous charge distribution near the α-ZrP/PPy interface can be attributed to the complex adsorption behaviors. Meanwhile, the charge is lost along the internal Li-S bond (green part) of Li_2S_4 and Li-S bond softens, which is consistent with the result of the lengthen of the Li-S bond. Beyond that, a large amount of charge accumulation on the P-O surface is clearly observed, which strongly supports that the charge is transferred remarkably from the LiPSs to the P-O surface along the Li-S bond, thus the LiPSs tend to be adsorbed on the active sites due to the charge accumulation. In contrast, the charge transfer merely happens between the S_8 cluster and

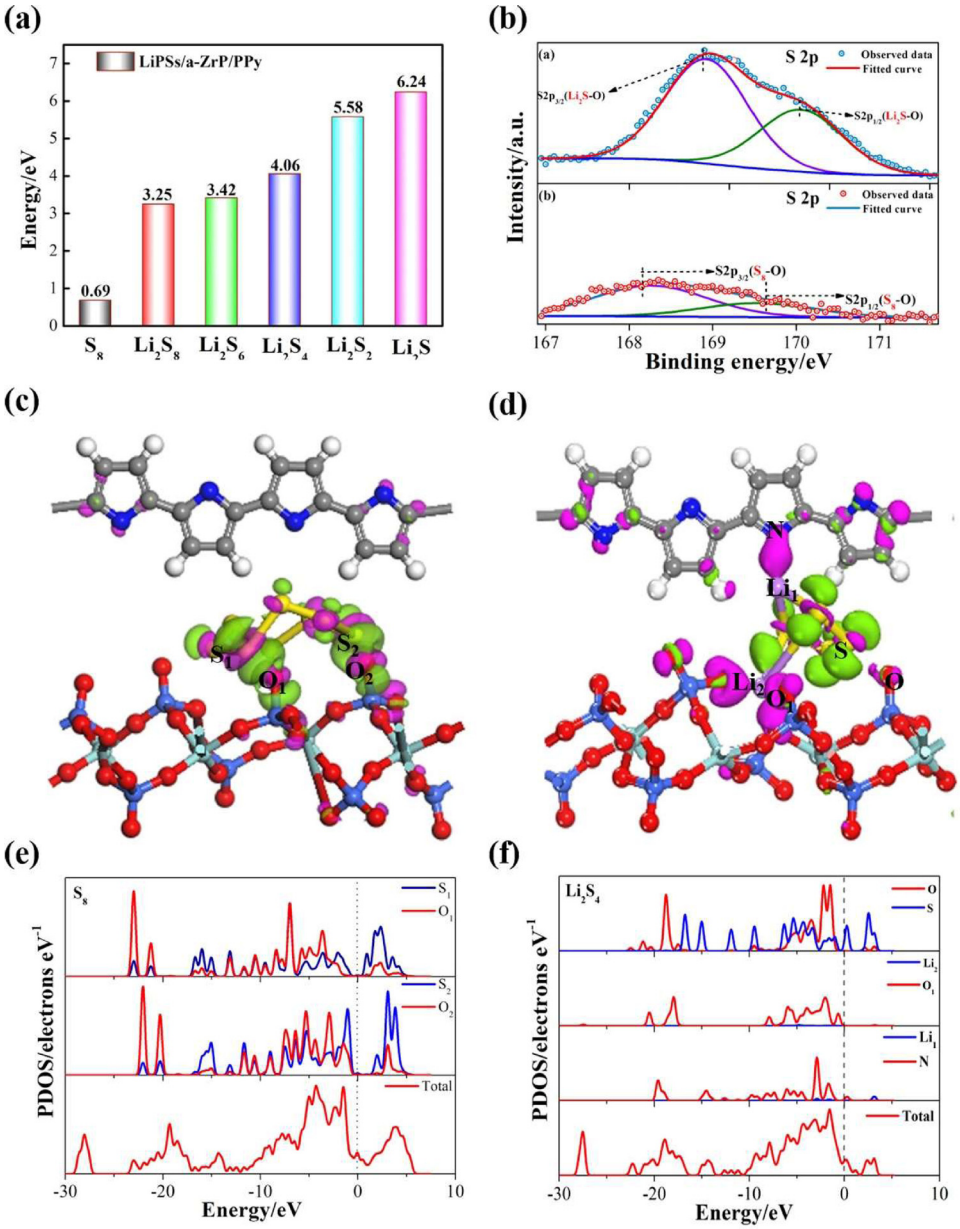

Fig. 6. (a) Binding energies for Li-S composites at six different lithiation stages (S_8, Li_2S_8, Li_2S_6, Li_2S_4, Li_2S_2, Li_2S) in α-ZrP/PPy interface. (b) XPS characterization of S 2p at charge (S_8)-discharge (Li_2S) states. (c,d) Electron density difference for S_8 and Li_2S_4 adsorption in α-ZrP/PPy with an isosurface of ±0.015 electrons Å^{-3}, where the pink and green isosurface represent the charge accumulation and depletion region, respectively. (e,f) Atomic partial density of states near the Fermi energy region for S_8 and Li_2S_4 clusters in the α-ZrP/PPy interface.

α-ZrP, indicating that the adsorption only comes from the effect of α-ZrP, which is also the reason why the adsorption energy of S_8 (−0.69 eV) drops sharply. Amazedly, it reveals an increased charge density between PPy and Li_2S_4 (pink part) together with the massive charges accumulation of P-O surface when Li_2S_4 is adsorbed in the α-ZrP/PPy system. Hereon, it can be considered that the introduction of a Li_2S_4 guest will open an electron transfer channel to feed back the electron from PPy to α-ZrP. Similarly, the α-ZrP withdraws even more electron of 1.59 e from the adsorption system, which is attributed to an electron-rich donor of α-ZrP. Furthermore, α-ZrP can serve as a moderate catalyst in enhancing the activity of P-O adsorption sites and accelerating the electrochemical reaction, which further indicates the chemical nature of substrate/Li_2S_n interaction. In brief, LiPSs act as the electronic switch to transfer the electrons from PPy to the surface of P-O, which would naturally generate much higher performance in the catalyzing of the Li_2S with rapid deposition; subsequently, PPy could hinder the output of electrons to avoid excessive oxidation of sulfide at the end of the charge process.

In addition, we analyzed the atomic partial density of states (*p*DOS) of the adsorption system near the Fermi energy to provide further insight into the nature of lithium bond and the chemical sulfur bond. Detailed results are shown in Fig. 6e with f and Fig. S2 of Supporting Information. Focusing on the red and blue curves, which represent the *p*DOS diagrams of O, S and Li atoms, intuitively, the positions of the Fermi level located in the pockets of the diverse atomic states, which refer to the different amounts of charge transfer [33]. The position of the Fermi level is consistent with the change in the amounts of electrons, which determines the adoption strengths of those LiPSs. As for Li_2S_4, the Fermi level is predominantly localized close to the left edge of the pocket of S atom, which results in a larger adsorption energy. While, for S_8, the

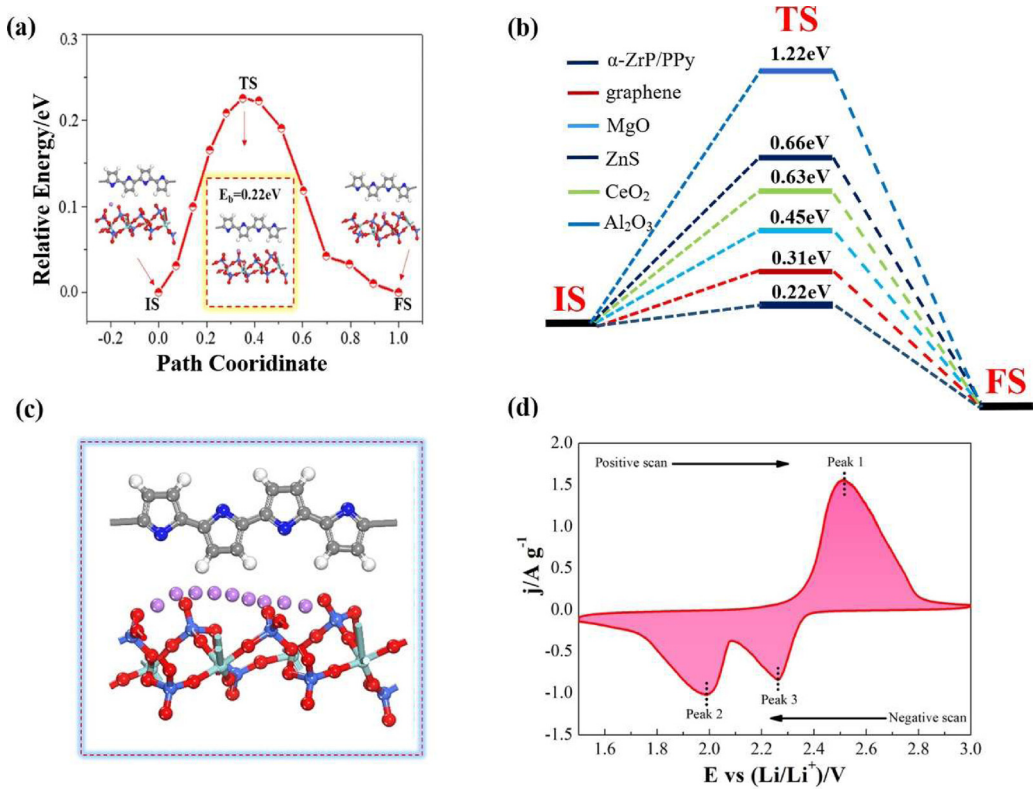

Fig. 7. (a) Transition state search of lithium ions diffusion in the α-ZrP/PPy interface with complete LST/QST method. (b) and compared with the previously reported cathode materials; (c) Lithium ions migration path diagram; (d) The relationship between the positions of the redox peaks of the two electrodes in the applied potential difference of 1.5 V to 3 V and the absolute current density.

Fermi level is located just outside the right edge of S atom, and the orbital is almost filled, thus the combination is very weak [33]. In addition, it can also be consciousd that there is almost no overlap between the *p*DOS of lithium atoms and oxygen atoms at the Fermi level whereas the *p*DOS of S-3p and O-2p have a well overlapped covering range, which stabilizes the adsorption of LiPSs. Moreover, by examining their density of states, as for Li atoms, there is only a minor contribution to the total density of states. On the contrary, the contribution of the density of states near the Fermi level is mainly derived from the S atoms, implying that the system forms true chemical sulfur bonds to retard the shuttle effect. Interestingly, it is discovered that the bandgap of the system approaches to zero when LiPSs are attached to the α-ZrP/PPy, and the simulated bandgap values are summarized in Table S2. Particularly, α-ZrP/PPy is transformed into a semiconductor-like state after Li_2S adsorption with the bandgap is changed from 0.08 to 0.04 eV even when Li_2S is identified as an electronic insulator. The electrical conductivity will be increased owing to the reduced bandgap, which correlates with the bandgap according to the Eq. (1). Hence, the conductivity of the system is 5 times higher than that of the previous one, which would dramatically improve the performance of Li-S batteries. That is, the higher conductivity of Li_2S or Li_2S_2 would accelerate the electron transport, thereby enhancing the LiPSs conversion process with the fleet charge compensation, indicating that α-ZrP/PPy plays an effective catalysis function in this process. Moreover, such a synergistic function effectively ensures that LiPSs can be smoothly captured and quickly converted, avoiding the shuttle effect and the sluggish kinetic reaction.

In order to deeply explore the existence of chemical sulfur bonds, XPS analysis was also performed [20]. As shown in Fig. 6b, for the original α-ZrP/PPy@S, the weak S characteristic peaks at 168.2 and 169.4 eV are attributed to the S-O bond of the weak chemical bond between α-ZrP and sulfur after the heat treatment. When α-ZrP/PPy@S is discharged to 1.5 V, a pair of new larger peaks appear in the spectrum, indicating the formation of a S-O bond. In this case, it is found that the conversion of sulfur was about 93.7%, signifying that α-ZrP/PPy has good chemical adsorption capacity with LiPSs, and the formed S-O bond will largely retard the shuttling effect. Furthermore, according to the theoretical simulation, the interlayer spacing is changed from 4.250 to 2.442 Å, which is stable enough to withstand the volume change of sulfur during the reaction, thereby significantly improving the performance of the Li-S battery.

3.3. Diffusion of lithium ion in the interface of α-ZrP/PPy

It is reported that the rate performance of the electrode material mainly depends on the mobility of Li ions [17,37]. Hence, it is important to quantify the diffusion of Li ions in α-ZrP/PPy interface. Herein, three kinds of diffusion paths are furnished, i.e., the diffusion of Li ions along the PPy direction, the diffusion of Li ions along the surface of α-ZrP, and the shuttle diffusion between PPy and α-ZrP. Based on the calculations, it is found that the PPy surface cannot provide the local minimum adsorption energy for the Li ion adsorption since Li ions will clip to the P-O surface after being completely relaxed. However, PPy provides the electron channel in the electrochemical reaction process while α-ZrP provides a dedicated ion slip transfer channel. Moreover, by carefully watching the video about the diffusion path of Li ions (as shown in the Support Information), it is found that P-O groups act as springboard to realize the rapid slippage of Li ions, resulting in the lengthening of Li-S bond. Fig. 7a-c show the structures and the energy profiles. Intuitively, Li ions follow an arc curve diffusing from one stable site to the next one in the α-ZrP/PPy interface, corresponding to a unimodal curve without metastable transition state. The calculation result demonstrates that the Li ion diffusion

Table 2
The computed relative energy barriers (Ea_1/Ea_2) and the relative diffusion migration (D_1/D_2) of lithium ion along α-ZrP@PPy (Ea_1, D_1) and other materials (Ea_2, D_2).

	Al_2O_3	ZnS	CeO_2	MgO	Graphene
Ea_1/Ea_2	11/61	1/3	22/63	22/45	22/31
D_1/D_2	7.735×10^{16}	2.697×10^{7}	8.399×10^{6}	7.662×10^{3}	33.110

barrier is 0.22 eV in the absence of an external electric field. Table 2 compares the α-ZrP/PPy with other materials [17,41]. Much larger magnitudes of the barriers, i.e., 0.31, 0.45, 0.63, 0.66 and 1.22 eV, at the same theoretical level are found for the diffusion along the graphene and other oxide substrate materials. To further elucidate the kinetics difference of various materials, the following Arrhenius Eq (3) is used:

$$D \sim \exp\left(-E_a k_B^{-1} T^{-1}\right) \quad (3)$$

Where D is the diffusion constant of Li ions [9,37], and E_a, k_B and T are the diffusion barrier and Boltzmann's constant, and temperature, respectively. It is estimated that at room temperature without an external electrical field, the diffusion mobility of Li ions in α-ZrP/PPy is approximately 10^{16} orders of magnitude faster than that of Al_2O_3 (Table 2). The lower barrier could lead to a faster diffusion rate, thereby accelerating the utilization of the active substrate and poor cycling [17]. Herein, the diffusion barrier is closely related to the adsorption strength and unique electronic properties, and a higher diffusion barrier indicates a redox reaction with more capacity. Briefly, as a material with electrochemically switched ion exchange property, the α-ZrP/PPy could catalyze the intercalation-deintercalation of lithium, by which sulfide could smoothly obtain those required ions for electrochemical reaction [17,21]. Meanwhile, the concentration of Li ions increases during the entire electrode reaction process, which would not only neutralize the redundant ions of surface but also eliminate the Faraday capacitance of the material. Consequently, the progressively decreasing energy barrier indicates that α-ZrP/PPy would be an excellent candidate for Li-S battery without losing much kinetic activity.

The cyclic voltammetry (CV) curve was employed to further investigate electrode kinetics with respect to the Li ions diffusion coefficient [41]. As shown in Fig. 7d, it is obvious that two reduction peaks appear at 1.98 and 2.26 V, corresponding to the formation of Li_2S_n and further reduction to Li_2S. The oxidation peak at 2.5 V is determined by the reverse conversion from Li_2S to S_8. The lower overpotential manifests the faster reaction kinetics of the battery after the incorporation of α-ZrP/PPy [20]. This finding further proves that α-ZrP/PPy is a potential ideal host material for Li-S batteries.

3.4. Decomposition of LiPSs in the interface of α-ZrP/PPy

During the charge-discharge cycle of Li-S batteries, the conversion from insoluble low-level LiPSs to high-level LiPSs and sulfur requires a large amount of activation energy, which will lead to a slow reaction rate. Insulating Li_2S_2/Li_2S deposited on the surface of the positive electrode could further generate the internal resistance of the battery. Therefore, the decomposition of LiPSs during the charging process is equally crucial. In order to understand the function of α-ZrP/PPy during the charging process and the reversibility of the battery, the decomposition barriers of five kinds of LiPSs were systematically studied to evaluate the kinetics reaction of delithiation on the surface [21].

In general, the catalytic oxidation of Li_2S is the first step, which is crucial for obtaining long cycle life and high reversible capacity [42]. During the battery charging process, since Li_2S has low conductivity, poor reversibility, and high charge transfer resistance,

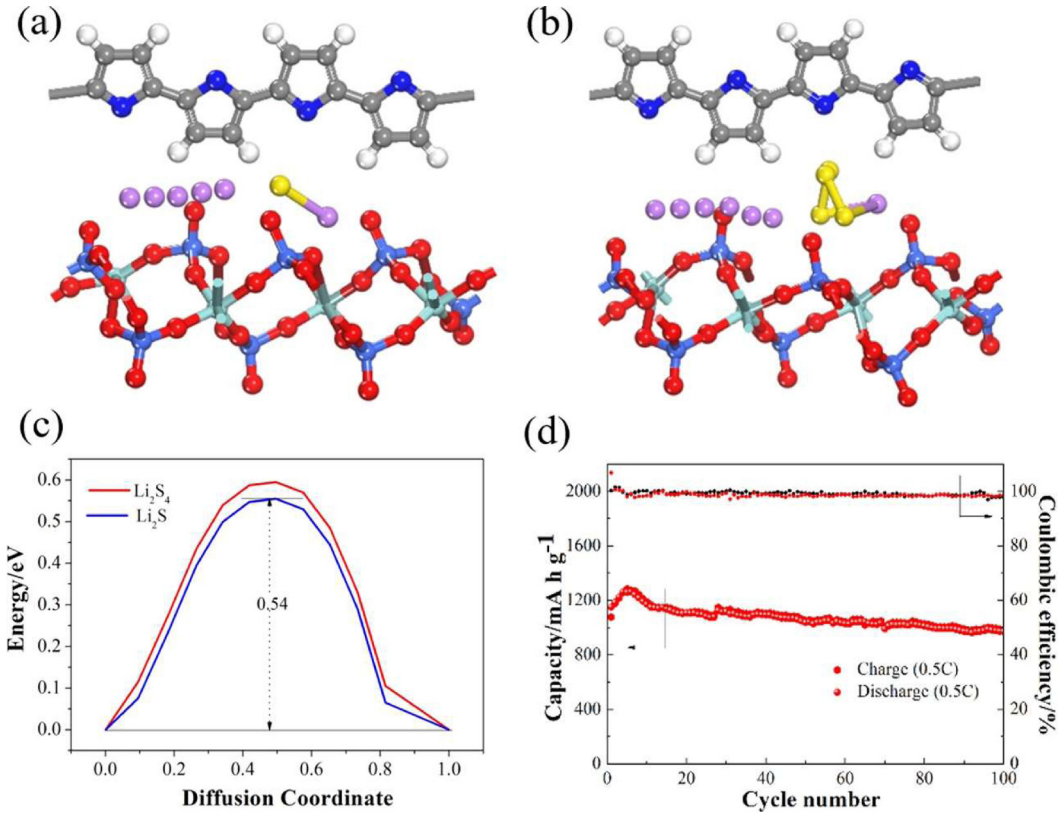

Fig. 8. (a,b) Corresponding decomposition pathways for Li_2S and Li_2S_4 adsorption in α-ZrP/PPy (c) Decomposition energy barriers of Li_2S and Li_2S_4 in the surface of α-ZrP/PPy during the charge process (d) Cycling stability of the α-ZrP/PPy@S composite at 0.5 C.

a high overpotential is needed to overcome the energy barrier. Herein, the complete decomposition of Li_2S molecule into a LiS cluster and a Li ion ($Li_2S \rightarrow LiS + Li^+ + e^-$) should occur [21]. It is worth noting that one Li ion could be located far away from S atom in this main evolution process for the adsorbed Li_2S system, resulting in the easily breaking of Li-S bonds (consistent with the previous research results). Taking Li_2S and Li_2S_4 as examples, the decomposition path of a Li ion is shown in Fig. 8a and b (others are demonstrated in Fig. S3 of the Supporting Information), and the energy profiles for the decomposition process of LiPSs are demonstrated in Fig. 8c. It can be clearly seen that the decomposition barriers of Li_2S and Li_2S_4 are as low as 0.54 and 0.59 eV, respectively, implying the transformation of insoluble Li_2S_2 and Li_2S towards soluble higher-order LiPSs would be closely related to the rapid Li ion diffusion. Compared with the decomposition barriers of other materials [21], α-ZrP/PPy shows a remarkably lower decomposition energy than others, which further confirms that α-ZrP/PPy is more kinetically favorable for LiPSs conversion and thereby realizing the reversibility of the battery (the corresponding calculation results are displayed in Fig. S4). Otherwise, long-chain Li_2S_6 and Li_2S_8 have much higher decomposition barriers of 2.20 and 2.50 eV, respectively, which could be attributed to the complete delithiation process and the continuous conversion needed to overcome a certain barrier to ensure the smooth redox, which is also an indicator of distinguished materials. In addition, it can be clearly observed that the decomposition barrier trend of LiPSs almost follows the same as the binding energy trend. That is, when the chemisorption between the intermediate and α-ZrP/PPy becomes stronger, the evolution process would have lower energy barrier. Surprisingly, based on the calculation results, it is found that the decomposition barrier of Li_2S_2 is 1.09 eV, which is not in line with the mentioned trend since the decomposition of Li_2S_n involves a complex phase transition process. Once the polar substrate is surrounded by LiPSs, the subsequent conversion of multiphase LiPSs will be hindered, and a higher barrier needs to overcome. Finally, the cycle stability performance diagram of α-ZrP/PPy was also investigated at a current density of 0.5 C. As shown in Fig. 8d, α-ZrP/PPy@S cathode exhibits an initial discharge capacity of 1150.3 mA h g^{-1} at 0.5 C over 100 cycles and a capacity retention of 84.3% is reached with excellent stability, which assists to adapt to the volume expansion of sulfur during the discharge process. Thus, the precious functionalization with the unique electrochemically switched ion exchange performance is to have a catalytic effect. That is to say, it plays a vital role in catalytic oxidation of short-order LiPSs to high-order LiPSs during battery charging as well as for sulfide binding and trapping, which is more advantageous for the sulfur utilization.

4. Conclusions

In conclusion, as an electrochemically switched ion exchange material, α-ZrP/PPy was designed as the sulfur host cathode to realize the smooth trapping-decomposition-conversion of LiPSs for suppressing the shuttle effect and facilitating kinetics redox reactions. This anchoring material integrates the merits of highly adsorptive ability of α-ZrP and high conductivity of PPy, by which LiPSs could be rapidly captured and then decomposed in the α-ZrP/PPy interface. As such, catalyzes the conversion of LiPSs could be effectively catalyzed, thereby realizing the reversibility of the battery. Meanwhile, it is considered that the LiPSs act as an electronic switch to transfer abundant electrons from α-ZrP to PPy, accelerating multi-phase transformation, improving sulfur utilization, and avoiding excessive oxidation of polysulfide. It is found that α-ZrP and PPy would supply unique ion migration channels and electronic transfer channels, respectively. Meanwhile, the α-ZrP/PPy has a relatively low lithium ions diffusion barrier owing to its ultra-high binding energy towards S_8 cluster and LiPSs as well as low decomposition barriers, which leads to ultra-long life of Li-S battery. In addition, such an anchoring material would maintain their metallic states during cycles, which adequately meets the obligations of fast kinetic reaction. This design concept for the sulfur cathode should propel the development of long-lifetime Li-S batteries.

Declaration of Competing Interest

The authors declare that they have no known competing financial interests or personal relationships that could have appeared to influence the work reported in this work.

Credit authorship contribution statement

Wei Zhang: Data curation, Investigation, Writing – original draft. **Ye Liu:** Methodology. **Ailian Wu:** Resources. **Lixia Ling:** Conceptualization. **Zhongde Wang:** Formal analysis, Funding acquisition. **Xiaogang Hao:** Supervision. **Guoqing Guan:** Writing – review & editing.

Acknowledgements

This original work was financially supported by the National Natural Science Foundation of China [grant number: 21878206]; the Science and Technology Innovation Project for Excellent Talents of Shanxi Province [grant number: 201805D211040]; the National Key R&D Program of China [grant number: 2017YFE0129200]; and the Fund Program for the Scientific Activities of Selected Returned Overseas Professionals of Shanxi Province in 2019.

Supplementary materials

Supplementary material associated with this article can be found, in the online version, at doi:10.1016/j.electacta.2021.139609.

References

[1] B. Kang, G. Ceder, Battery materials for ultrafast charging and discharging, Nat. 458 (2009) 190–193, doi:10.1038/nature07853.
[2] Y.M. Chiang, Materials science, building a better battery, Sci 330 (2010) 1485–1486, doi:10.1126/science.1198591.
[3] K. Zhao, W.L. Wang, J. Gregoire, P. Matt, Z.G. Suo, J.V. Joost, K. Efthimios, Lithium-assisted plastic deformation of silicon electrodes in lithium-ion batteries: a first-principles theoretical study, Nano Lett. 11 (2011) 2962–2967, doi:10.1021/nl201501s.
[4] J.B. Goodenough, K.S. Park, The Li-ion rechargeable battery: a prspective, J. Am. Chem. Soc. 135 (2013) 1167–1176, doi:10.1021/ja3091438.
[5] S. Evers, L.F. Nazar, New approaches for high energy density lithium-sulfur battery cathodes, Acc. Chem. Res. 46 (2013) 1135–1143, doi:10.1021/ar3001348.
[6] T. Yu, F. Li, C. Liu, S. Zhang, H. Xu, G. Yang, Understanding the role of lithium sulfide clusters in lithium-sulfur batteries, J. Mater. Chem. A 5 (2017) 9293–9298, doi:10.1039/C7TA01006K.
[7] H. Yuan, W. Zhang, J.G. Wang, G.M. Zhou, Z.Z. Zhuang, J.M. Luo, H. Huang, Y.P. Gan, C. Liang, Y. Xia, J. Zhang, X.Y. Tao, Facilitation of sulfur evolution reaction by pyridinic nitrogen doped carbon nanoflakes for highly-stable lithium-sulfur batteries, Energy Storage Mater 10 (2018) 1–9, doi:10.1016/j.ensm.2017.07.015.
[8] Z. Li, H.B. Wu, X.W. Lou, Rational designs and engineering of hollow micro-/nanostructures as sulfur hosts for advanced lithium-sulfur batteries, Energy Environ. Sci. 9 (2016) 3061–3070, doi:10.1039/C6EE02364A.
[9] T.T. Li, C. He, W.X. Zhang, A novel porous C4N4 monolayer as a potential anchoring material for lithium-sulfur battery design, J. Mater. Chem. A 7 (2019) 4134–4144, doi:10.1039//c8ta109 3h.
[10] S.M. Zhang, Q. Zhang, J.Q. Huang, X.F. Liu, W.C. Zhu, M.Q. Zhao, W.Z. Qian, F. Wei, Composite cathodes containing SWCNT@S coaxial nanocable: facile synthesis, surface modification, and enhanced performance for Li-ion storage, Part. & Part. Syst. Char. 30 (2013) 158–165, doi:10.1002/ppsc.201200082.
[11] H.J. Peng, T.Z. Hou, Q. Zhang, J.Q. Huang, X.B. Cheng, M.Q. Guo, Z. Yuan, L.Y. He, F. Wei, Strongly coupled interfaces between a heterogeneous carbon host and a sulfur-containing guest for highly stable lithium-sulfur batteries: mechanistic insight into capacity degradation, Adv. Mater. Interfaces 1 (2014) 1400227–1400236, doi:10.1002/admi.201400227.
[12] R. Elazari, G. Salitra, A. Garsuch, A. Panchenko, D. Aurbach, Sulfur-impregnated activated carbon fiber cloth as a binder-free cathode for rechargeable Li-S batteries, Adv. Mater. 23 (2011) 5641–5644, doi:10.1002/adma.201103274.

[13] J.Q. Huang, X.F. Liu, Q. Zhang, C.M. Chen, M.Q. Zhao, S.M. Zhang, W.C. Zhu, W.Q. Zhong, F. Wei, Entrapment of sulfur in hierarchical porous graphene for lithium-sulfur batteries with high rate performance from -40 to 60°C, Nano Energy 2 (2013) 314–321, doi:10.1016/j.nanoen.2012.10.003.
[14] W.Y. Li, Q.F. Zhang, G.Y. Zheng, Z.W. Seh, H.B. Yao, Y. Cui, Understanding the role of different conductive polymers in improving the nanostructured sulfur cathode performance, Nano Lett 13 (2013) 5534–5540, doi:10.1021/nl403130h.
[15] J.X. Song, M.L. G.ordin, T. Xu, S.R. Chen, Z.X. Yu, H. Sohn, J. Lu, Y. Ren, Y.H. Duan, D.H. Wang, Strong lithium polysulfide chemisorption on electroactive sites of nitrogen-doped carbon composites for high-performance lithium-sulfur battery cathodes, Angew. Chem. Int. Ed. 54 (2015) 4325–4329, doi:10.1002/ange.201411109.
[16] T.Z. Hou, X. Chen, H.J. Peng, J.Q. Huang, B.Q. Li, Q. Zhang, B. Li, Design principles for heteroatom-doped nanocarbon to achieve strong anchoring of polysulfides for lithium-sulfur batteries, Small 12 (2016) 3283–3291, doi:10.1002/smll.201600809.
[17] X. Chen, H.J. Peng, R. Zhang, T.Z. Hou, J.Q. Huang, B. Li, Q. Zhang, An analogous periodic law for strong anchoring of polysulfides on polar hosts in lithium sulfur batteries: S or Li binding on first-row transition-metal sulfides? ACS Energy Lett. 2 (2017) 795–801, doi:10.1021/acsenergyl ett.7b00164.
[18] Z.W. Seh, W.Y. Li, J.J. Cha, G.Y. Zheng, Y. Yang, M.T. McDowell, P.C. Hsu, Y. Cui, Sulphur-TiO_2 yolk-shell nanoarchitecture with internal void space for long-cycle lithium-sulphur batteries, Nat. Commun. 4 (2013) 1331–1336, doi:10.1038/ncomms2327.
[19] Q. Fan, W. Liu, Z. Weng, Y.M. Sun, H.L. Wang, Ternary hybrid material for high-performance lithium-sulfur battery, J. Am. Chem. Soc. 137 (2015) 12946–12953, doi:10.1021/jacs.5b07071.
[20] X. Wu, N.N. Liu, M.X. Wang, Y. Qiu, B. Guan, D. Tian, Z.K. Guo, L.S. Fan, N.Q. Zhang, A class of catalysts of BiOX (X = Cl, Br, I) for anchoring polysulfides and accelerating redox reaction in lithium sulfur batteries, ACS Nano 13 (2019) 13109–13115, doi:10.1021/acsnano. 9b05908.
[21] G.M. Zhou, H.Z. Tian, Y. Jin, X.Y. Tao, B.F. Liu, R.F. Zhang, W.Z. S.he, D. Zhuo, Y.Y. Liu, J. Sun, J. Zhao, C.X. Zu, D.S. Wu, Q.F. Zhang, Y. Cui, Catalytic oxidation of Li_2S on the surface of metal sulfides for Li-S batteries, P. Natl. A. Sci. 114 (2017) 840–845, doi:10.1002/adfm. 201707234.
[22] Z. Yuan, H.J. Peng, T.Z. Hou, J.Q. Huang, C.M. Chen, D.W. Wang, X.B. Cheng, F. Wei, Q. Zhang, Powering lithium-sulfur battery performance by propelling polysulfide redox at sulfiphilic hosts, Nano Lett 16 (2016) 519–527, doi:10.1002/adma.201501559.
[23] H.L. Pan, K.S. Han, M.H. Engelhard, R.G. Cao, J.Z. Chen, J.G. Zhang, K.T. Mueller, Y.Y. Shao, J. Liu, Addressing passivation in lithium-sulfur battery under lean electrolyte condition, Adv. Func. Mater. 28 (2018) 1707234–1707241, doi:10.1073/pnas.1615837114.
[24] F.Y. Fan, W.C. Carter, Y.M. Chiang, Mechanism and kinetics of Li2S precipitation in lithium-sulfur batteries, Adv. Mater. 27 (2015) 5203–5209, doi:10.1002/adma.201501559.
[25] Z.D. Wang, Y.T. Feng, X.G. Hao, W. Huang, X.S. Feng, A novel potential-responsive ion exchange film system for heavy metal removal, J. Mater. Chem. A 2 (2014) 10263–10272, doi:10.1039/c4ta00782d.
[26] X.S. Lv, W. Wei, H.C. Yang, J.J. Li, B.B. Huang, Y. Dai, Group IV monochalcogenides MX (M = Ge, Sn; X = S, Se) as chemical anchors of polysulfides for lithium-sulfur batteries, Chem 24 (2018) 11193–11199, doi:10.1002/cssc.201902227.
[27] X. Du, Q. Zhang, W.L. Qiao, X.L. Sun, X.L. Ma, X.G. Hao, Z.D. Wang, A. Abudula, G.Q. Guan, Controlled self-assembly of oligomers-grafted fibrous polyaniline/single zirconium phosphate nanosheet hybrids with potential-responsive ion exchange properties, Chem. Eng. J. 302 (2016) 516–525, doi:10.1002/chem.201801925.
[28] Q. Zhang, X. Du, X.L. Ma, X.G. Hao, G.Q. Guan, Z.D. Wang, C.F. Xue, Z.L. Zhang, Z.J. Zuo, Facile preparation of electroactive amorphous alpha-ZrP/PANI hybrid film for potential-triggered adsorption of Pb2+ ions, J. Hazard Mater. 289 (2015) 91–100, doi:10.1016/j.cej.2016.05.066.
[29] Y. Liu, W.J. Yan, W. Zhang, W. Kong, Z.D. Wang, X.G. Hao, G.Q. Guan, 2D sandwich-like alpha-zirconium phosphate/polypyrrole: moderate catalytic activity and true sulfur confinement for high-performance lithium-sulfur batteries, ChemSusChem 12 (2019) 5172–5182, doi:10.1002/cssc.201902227.
[30] S.J. Clark, M.D. Segall, C.J. Pickard, P.J. Hasnip, M.I.J. Probert, K. Refson, M.C. Payne, First principles methods using CASTEP, Z, Krist-Cryst Mater. 220 (2005) 567–570, doi:10.1524/zkri.220.5.567.65075.
[31] J.P. Perdew, K. Burke, M. Ernzerhof, Generalized gradient approximation made simple, Phys. Rev. Lett. 77 (1996) 3865–3868, doi:10.1103/PhysRevLett.77.3865.
[32] B. Delley, An all?electron numerical method for solving the local density functional for polyatomic molecules, J. Chem. Phys. 92 (1990) 508–517, doi:10.1063/1.458452.
[33] Q.F. Zhang, Y.P. Wang, Z.W. Seh, Z.H. Fu, R.F. Zhang, Y. Cui, Understanding the anchoring effect of two-dimensional layered materials for lithium-sulfur batteries, Nano Lett. 15 (2015) 3780–3786, doi:10.1021/acs.nanolett.5b00367.
[34] D. Vanderbilt, Soft self-consistent pseudopotentials in a generalized eigenvalue formalism, Phys. Rev. B Condens. Matter Mater. Phys. 41 (1990) 7892–7895, doi:10.1103/PhysRevB.41.789 2.
[35] H. Ushiyama, Theoretical studies on membranes and non-platinum catalysts for polymer electrolyte fuel cells, AIP Conf. Proc. 1702 (2015) 090045 090045-3, doi:10.1063/1.4938853.
[36] N. Govind, M. Petersen, G. Fitzgerald, D. King-Smith, J. Andzelm, A generalized synchronous transit method for transition state location, Comp. Mater. Sci. 28 (2003) 250–258, doi:10.1016/S0927-0256(03)00111-3.
[37] Y. Jing, Z. Zhou, C.R. Cabrera, Z.F. Chen, Metallic VS2 monolayer: a promising 2D anode material for lithium ion batteries, J. Phys. Chem. C 117 (2013) 25409–25413, doi:10.1021/jp410969u.
[38] J.X. Zhao, Y.A. Yang, R.S. Katiyar, Z.F. Chen, Phosphorene as a promising anchoring material for lithium-sulfur batteries: a computational study, J. Mater. Chem. A 4 (2016) 6124–6130, doi:10.1039/C6TA00871B.
[39] Y. Wu, B. Zhu, M. Huang, L. Liu, Q. Shi, M. Akbar, C. Chen, J. Wei, J.F. Li, L.R. Zheng, J.S. Kim, H.B. Song, Proton transport enabled by a field-induced metallic state in a semiconductor heterostructure, Sci 369 (2020) 184–188, doi:10.1126/science.aaz9139.
[40] C. Ataca, E. Aktürk, S. Ciraci, H. Ustunel, High-capacity hydrogen storage by metallized graphene, Appl. Phys. Lett. 93 (2008) 043123–043123-3, doi:10.1063/1.2963976.
[41] X.Y. Tao, J.G. Wang, C. Liu, H.T. Wang, H.B. Yao, G.Y. Zheng, Z.W. She, Q.X. Cai, W.Y. Li, G.M. Zhou, C.X. Zu, Y. Cui, Balancing surface adsorption and diffusion of lithium-polysulfides on nonconductive oxides for lithium-sulfur battery design, Nat. Commun. 7 (2016) 11203–11211, doi:10.1038/ncomms11203.
[42] W.J. Cui, S.S. Yu, J.X. Zhao, Two-dimensional ?-conjugated metal bis (dithiolene) nanosheet: a promising anchoring material for lithium-sulfur batteries, Comp. Mater. Sci. 171 (2020) 109228–109236, doi:10.1016/j.commatsci.2019.109228.